Hindawi
International Transactions on Electrical Energy Systems
Volume 2022, Article ID 7041778, 16 pages
https://doi.org/10.1155/2022/7041778

Research Article

Research on Economic Optimal Dispatching of Microgrid Cluster Based on Improved Butterfly Optimization Algorithm

Yu Zhang,[1,2] **Hui Zhou**,[1] **Liexi Xiao**,[1] **and Guanhao Zhao**[1]

[1]*College of Mechanical and Control Engineering, Guilin University of Technology, Guilin 541004, China*
[2]*Guangxi Key Laboratory of Building New Energy and Energy Saving, Guilin 541004, China*

Correspondence should be addressed to Yu Zhang; 17316606@qq.com

Received 8 November 2021; Revised 2 December 2021; Accepted 13 December 2021; Published 31 January 2022

Academic Editor: Faroque Azam

Microgrid optimal dispatching has become one of the core issues of microgrid energy management and integrated control, which is of great significance to reduce energy consumption and environmental pollution. As a natural heuristic algorithm, the butterfly optimization algorithm (BOA) has the advantages of simple adjustment parameters and fast convergence speed. It is widely used to solve nonlinear programming problems. However, BOA is easy to fall into local optimization and poor convergence accuracy. Therefore, an improved butterfly optimization algorithm (IBOA) based on skew tent chaotic map, Cauchy mutation, and simplex method is proposed, and compared with particle swarm optimization (PSO), whale optimization algorithm (WOA), sparrow search algorithm (SSA), and BOA, the results show that the IBOA has high convergence speed and optimization accuracy. Finally, the IBOA is used to solve the optimization model. The simulation results show that the IBOA can effectively reduce the power consumption cost of the system, promote the effective utilization of renewable energy, and improve the operation stability of the microgrid cluster system.

1. Introduction

Nonrenewable energy plays a crucial role as the main energy in production and life. However, due to the overexploitation of nonrenewable energy, a series of problems caused by the use of nonrenewable energy is gradually expanding, endangering the ecological environment of the natural world, and the development and utilization of renewable energy such as wind energy and solar energy are becoming more and more important. With the development of renewable energy and energy storage batteries, the microgrid cluster system consisting of multiple microgrids can make effective use of renewable energy and has good development prospects [1–4]. The microgrid cluster system is an extension of the microgrid system. Compared with a single microgrid, the interconnected operation of multiple microgrids not only improves the reliability of the power supply but also plays an important role in reducing power economic costs and environmental protection. Microgrid optimal dispatch problem is generally multi-objective optimization. Due to the random fluctuation of distributed energy, the microgrid optimal dispatch problem has become a nonlinear, multi-constrained, multivariable combinatorial optimization problem [5–8]. For traditional algorithms, it is usually hard to find a feasible or optimal solution. In recent years, biomimetic-inspired intelligent optimization algorithms have become increasingly important in solving the optimal dispatch problem of the microgrid [9, 10]. Popular algorithms such as PSO [11, 12], genetic algorithm (GA) [13, 14], and ant colony optimization (ACO) [15] have better global optimization ability and robustness.

At present, many scholars have done a lot of research on the optimal dispatch of the microgrid. Miao et al. [16] proposed a cost-benefit model for analyzing the scale of microgrid energy storage system (ESS), which is solved by the gray wolf optimization (GWO). The superiority of intelligent optimization algorithms in solving microgrid optimal dispatch problems was verified, but the convergence speed of GWO was slow when solving the model. Alireza et al. [17] proposed an off-grid microgrid model consisting of photovoltaics (PV), wind turbine (WT), micro-turbine (MT), ESS, and gas boiler (GB), which took the annual total cost as the objective function and was solved by evolutionary particle swarm optimization (E-PSO). Compared with other intelligent algorithms, the results showed that E-PSO has better searching ability than other algorithms, but it may fall into local optimum when solving high-dimensional nonlinear programming problems. In Reference [18], the optimal size of the ESS in the microgrid was analyzed and solved by PSO, GA, and flower pollination algorithm (FPA). Although the optimal solution was obtained, the initial algorithms are prone to falling into the local optimization problem, and a more accurate value can be obtained by improving the algorithm. In Reference [19], an optimal system configuration model for determining a reliable power supply system was proposed and solved using the grasshopper optimization algorithm (GOA). The results showed that the GOA outperformed the cuckoo search (CS) and PSO in terms of searching ability, but that there is still room for improvement. Abhilipsa et al. [20] proposed a microgrid bidding strategy model in an uncontrolled environment and solved it using an improved whale optimization algorithm (IWOA). Compared with WOA, PSO, and bat algorithm (BA), although the overall economic cost has been optimized, the impact of environmental costs has not been taken into account. Zahraoui et al. [21] determined the optimal generation capacity of distributed power with the objective of the lowest total generation cost and solved it using a memory-based gravitational search algorithm (MBGSA). Compared with GSA, artificial bee colony (ABC), GA, and PSO, the cost of generating electricity has been reduced, but the environmental costs of distributed power sources have not been taken into account. Soheil et al. [22] used the levy-flight moth-flame optimization algorithm (LMFOA) to solve the problem with the objective of minimizing the life cost of internal equipment and the transaction cost of electricity in the microgrid. Compared with MFOA, hybrid genetic algorithm and particle swarm algorithm, and ACO, the superiority of the improved algorithm was verified, but only a single microgrid system was considered, and the microgrid group system composed of multiple microgrids was not considered. Morteza et al. [23] proposed a model to determine the optimal size of the ESS with the lowest total cost as the objective, solved it by convex optimization, and compared it with GA and PSO. The power interaction in grid-connected situations was not considered, although the lowest total cost was obtained.

In summary, most of the research on optimal dispatch of microgrids still stays at the level of a single microgrid. The microgrid cluster system composed of multiple microgrids can make up for the insufficiencies of fluctuation, indirectness, and randomness of distributed power supply, effectively improve the stability of the system, and reduce the rate of light and wind abandonment, so the optimal dispatch research on microgrid cluster is particularly important. In this study, a microgrid cluster system model composed of three microgrids is constructed, which considers the generation cost, equipment operation and maintenance cost, ESS operation cost, energy transaction cost, and environmental cost of the power generation unit, and uses IBOA to simulate and solve the model. To improve the searchability of the algorithm, a skew tent chaotic map is used to improve population diversity, and then, the Cauchy mutation is used in the search process to change the location information of butterflies, expand the search space, and finally use the simplex method to improve the poor individuals in the location update process. As a result, the microgrid cluster's optimum dispatch may be solved more efficiently.

2. Economic Dispatching Model of Microgrid Cluster

2.1. Microgrid Cluster System Structure. The microgrid cluster is composed of several microgrids, each of which is an individual, including PV, WT, diesel generator (DG), MT, ESS, and load. The interaction between the microgrid cluster and the distribution network is carried out through the information interaction center, as shown in Figure 1.

2.2. Objective Function. The objective function is to minimize the operating cost and environmental cost of the microgrid cluster. The operating cost includes the generation cost of controllable distributed generating units, the operation and maintenance cost of generating equipment, the operation cost of ESS, and the transaction cost of electricity. The environmental cost is the penalty cost for pollutant gases (CO_2, SO_2, and NO_x), and the objective function is to maximize the overall benefits of the microgrid cluster. The specific objective functions can be represented as follows:

$$C = C_1 + C_2, \tag{1}$$

$$C_1 = \sum_{i=1}^{n}\sum_{t=1}^{24}\left[C_i^{\mathrm{DG}}(t) + C_i^{\mathrm{MT}}(t) + C_i^{\mathrm{EM}}(t) + C_i^{\mathrm{ESS}}(t) + C_i^{\mathrm{ET}}(t)\right], \tag{2}$$

$$C_2 = \sum_{i=1}^{n}\sum_{t=1}^{24}\sum_{k=1}^{3}\left[C_k\lambda_k^{\mathrm{DG}}P_i^{\mathrm{DG}}(t) + C_k\lambda_k^{\mathrm{MT}}P_i^{\mathrm{MT}}(t) + C_k\lambda_k^{\mathrm{grid}}P_i^{\mathrm{buy}}(t)\right], \tag{3}$$

where C_k is the cost factor for handling K-type pollutants, and there are three main pollutants (CO_2, SO_2, and NO_x).

2.2.1. Cost of Diesel Generator. The cost of DG is related to fuel consumption and can be expressed as follows:

$$C_i^{\mathrm{DG}}(t) = \alpha\left[P_i^{\mathrm{DG}}(t)\right]^2 + \beta P_i^{\mathrm{DG}}(t) + \gamma, \tag{4}$$

where α, β, and γ are the fuel consumption cost factors of the DG. Typically, $\alpha = 0.001$, $\beta = 0.18$, and $\gamma = 6$ [24].

2.2.2. Cost of Micro-Turbine. The cost of MT is related to gas consumption and can be represented as follows:

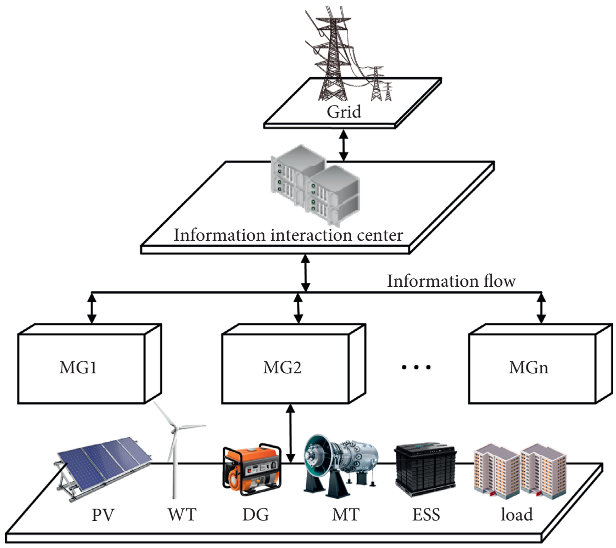

Figure 1: Microgrid cluster diagram.

$$C_i^{\mathrm{MT}}(t)=\frac{C_{\mathrm{nl}}}{L}\times\frac{P_i^{\mathrm{MT}}(t)}{\eta_i^{\mathrm{MT}}(t)},\tag{5}$$

where C_{nl} is the price of natural gas, L is the low calorific value of natural gas, P_i^{MT} is the power of MT, and η_i^{MT} is the power generation efficiency of MT [25]. Typically, $C_{\mathrm{nl}}=2.5$ CNY/m^3 and $L=9.7$KWh/m^3.

2.2.3. Maintenance Cost of Power Generation Equipment. The power generation equipment will cause some loss during operation, which can be expressed as follows:

$$\begin{aligned}C_i^{\mathrm{EM}}(t)&=k_i^{\mathrm{WT}}(t)P_i^{\mathrm{WT}}(t)+k_i^{\mathrm{PV}}(t)P_i^{\mathrm{PV}}(t)+k_i^{\mathrm{DG}}(t)P_i^{\mathrm{DG}}(t)\\&\quad+k_i^{\mathrm{MT}}(t)P_i^{\mathrm{MT}}(t).\end{aligned}\tag{6}$$

2.2.4. Operation Cost of Energy Storage System. Due to the randomness and fluctuation of distributed power supply, the ESS discharges when the power generation is insufficient, charges when the power generation is sufficient, and produces a certain loss when charging and discharging, which can be expressed as follows:

$$C_i^{\mathrm{ESS}}(t)=\frac{C_i^{\mathrm{cost}}}{P_i^{\mathrm{R}}T}\times\frac{d_i\left(1+d_i\right)^{l_i}}{\left(1+d_i\right)^{l_i}-1}P_i^{\mathrm{ESS}}(t).\tag{7}$$

2.2.5. Transaction Cost of Electricity. There are costs incurred when the microgrid trades with the microgrid and the microgrid trades with the distribution network, which can be expressed as follows:

$$C_i^{\mathrm{ET}}(t)=P_i^{\mathrm{mg}}(t)\delta_i^{\mathrm{mg}}(t)+P_i^{\mathrm{grid}}(t)\delta_i^{\mathrm{grid}}(t),\tag{8}$$

where P_i^{mg} and P_i^{grid} are positive when purchasing electricity and negative when selling electricity.

2.3. Constraints. When optimizing the microgrid cluster system, the following constraints need to be considered.

2.3.1. Power Balance Constraint. This constraint is for the total power of the microgrid cluster system and plays an important role in optimal dispatch, which can be expressed as follows:

$$\begin{aligned}&P_i^{\mathrm{WT}}(t)+P_i^{\mathrm{PV}}(t)+P_i^{\mathrm{DG}}(t)+P_i^{\mathrm{MT}}(t)+P_i^{\mathrm{ESS}}(t)+P_i^{\mathrm{mg}}(t)\\&\quad+P_i^{\mathrm{grid}}(t)=P_i^{\mathrm{load}}(t).\end{aligned}\tag{9}$$

2.3.2. Power Generation Equipment Constraints. This restriction is mainly derived from the physical constraints of the power generation equipment and can be expressed as follows:

$$R_{i,\mathrm{down}}^{\mathrm{DG}}\Delta t\le P_i^{\mathrm{DG}}(t)-P_i^{\mathrm{DG}}(t-1)\le R_{i,\mathrm{up}}^{\mathrm{DG}}\Delta t,\tag{10}$$

$$R_{i,\mathrm{down}}^{\mathrm{MT}}\Delta t\le P_i^{\mathrm{MT}}(t)-P_i^{\mathrm{MT}}(t-1)\le R_{i,\mathrm{up}}^{\mathrm{MT}}\Delta t.\tag{11}$$

2.3.3. Energy Storage System Constraints. The energy storage systems can improve the stability of microgrid cluster, and the constraints can be expressed as follows:

(1) Charge state constraint

$$\mathrm{SOC}_i^{\min}\le\mathrm{SOC}(t)\le\mathrm{SOC}_i^{\max}.\tag{12}$$

(2) Power constraints for charging and discharging

$$\begin{cases}0\le P_i^{\mathrm{ch}}(t)\le P_i^{\max},\\0\le P_i^{\mathrm{dis}}(t)\le P_i^{\max},\\P_i^{\mathrm{ch}}(t)\times P_i^{\mathrm{dis}}(t)=0.\end{cases}\tag{13}$$

3. Proposed Enhancements for Butterfly Optimization Algorithm

3.1. Butterfly Optimization Algorithm. The BOA is a natural heuristic algorithm proposed for the feeding behavior of butterflies. In BOA, all butterflies attract each other by emitting some fragrance. Each butterfly moves randomly or toward the best butterflies and emits more fragrance [26]. The size of the butterfly aroma is a function of the physical intensity of the stimulus, and the formula can be expressed as follows:

$$f=cI^{\alpha},\tag{14}$$

where f is the aroma size of butterflies, c is the sensory modality, I is the stimulation intensity, and α is the power exponent with a range of [0,1].

The location update formula for the global search phase can be expressed as follows:

$$x_i^{t+1}=x_i^t+\left(r^2\times g^*-x_i^t\right)\times f_i,\tag{15}$$

where x_i^t is the position vector of the ith butterfly in the tth iteration, r is the random number between [0,1], g^* is the current optimal solution, and f_i is the aroma size of the ith butterfly.

The location update formula for the local search phase can be expressed as follows:

$$x_i^{t+1} = x_i^t + \left(r^2 \times \left(x_j^t - x_k^t\right) - x_i^t\right) \times f_i, \tag{16}$$

where x_j^t and x_k^t refer to the position vectors of the jth and kth individuals randomly selected from within the population in the tth iteration, respectively.

Global and local searches occur when a butterfly is searching for food and are determined by setting the switch probability p.

3.2. Improved Butterfly Optimization Algorithm

3.2.1. Chaotic Map Initialization Population. Chaotic sequences generated by chaotic mapping have the advantages of randomness, traversal, non-repeatability, etc. In the optimization field, they are often used to generate the initial position of the population, which can effectively improve the diversity of the population. Here, the skew tent chaotic mapping is used to initialize butterfly population, and its definition can be expressed as follows:

$$x_{n+1} = \begin{cases} \dfrac{x_n}{\alpha}, & x_n < \alpha, \\ \dfrac{1 - x_n}{1 - \alpha}, & x_n \geq \alpha, \end{cases} \tag{17}$$

where α is a random number from 0 to 1.

3.2.2. Cauchy Variation. The Cauchy density function is similar to the Gauss density function, but the Cauchy distribution has a higher two-wing probability characteristic, a wider distribution range than the random numbers generated by the Gauss distribution, which effectively improves the global searchability of the algorithm and makes it easy to jump out of the local optimum [27]. The Cauchy distribution function can be expressed as follows:

$$F_t(x) = \frac{1}{2} + \frac{1}{\pi}\arctan\left(\frac{x}{t}\right), \tag{18}$$

where t is a proportional function and has a positive value.

The Cauchy operator is introduced in the global search and local search to mutate individual locations, which makes it easier for the algorithm to jump out of the local optimal value and improve the accuracy of the algorithm.

The location of the global search phase is updated as follows:

$$x_i^{t+1} = x_i^t + \left(r^2 \times g^* - x_i^t\right) \times f_i \times \mathrm{Cauchy}(0, 1). \tag{19}$$

The location of the local search phase is updated as follows:

$$x_i^{t+1} = x_i^t + \left(r^2 \times \left(x_j^t - x_k^t\right) - x_i^t\right) \times f_i \times \mathrm{Cauchy}(0, 1). \tag{20}$$

3.2.3. Simplex Method. The advantages of the simplex method include a simple principle, small computation, quick convergence, and strong local searchability. It can effectively improve the local development ability and search accuracy of BOA. The simplex method entails creating $n+1$ vertex polyhedrons in n-dimensional space, calculating and comparing the fitness values of each vertex, and determining the best, second best, and worst points. By reflection, expansion, contraction, and other strategies, a better advantage is obtained, and a new polyhedron is formed, iterating and approaching the optimal point gradually. The steps can be expressed as follows:

Step 1: calculate the fitness values of all vertices, rank the individual fitness values, and determine the optimal point x_1, the secondary advantage x_2, and the worst point x_3.

Step 2: calculates the center point of the optimal point x_1 and the secondary advantage x_2, which is counted as x_4.

Step 3: reflect the worst point x_3 to get the reflection point, which is recorded as x_5 and can be expressed as follows:

$$x_5 = x_4 + \alpha\left(x_4 - x_3\right), \tag{21}$$

where α is the reflection coefficient in the formula and the value is 1.

Step 4: if $f(x_5) < f(x_1)$, the reflection direction is correct, the expansion operation is performed, and the expansion point is obtained, which is recorded as x_6 and can be expressed as follows:

$$x_6 = x_4 + \beta\left(x_5 - x_4\right), \tag{22}$$

where β is the expansion factor and the value is 1.5.

If $f(x_6) < f(x_1)$, the worst point x_3 is replaced by the expansion point x_6; otherwise, the worst point x_3 is replaced by the reflection point x_5.

Step 5: if $f(x_5) > f(x_1)$, the reflection direction is incorrect. Compression is performed to get the compression point, which is recorded as x_7 and can be expressed as follows:

$$x_7 = x_4 + \gamma\left(x_3 - x_4\right), \tag{23}$$

where γ is the compression factor and the value is 0.5.

If $f(x_7) < f(x_3)$, the worst point x_3 is replaced by the compression point x_7.

Step 6: if $f(x_1) < f(x_5) < f(x_3)$, a contraction operation is performed to get the contraction point, which is recorded as x_8 and can be expressed as follows:

$$x_8 = x_4 - \varepsilon\left(x_3 - x_4\right), \tag{24}$$

where ε is the shrinkage factor and the value is 0.5.

Table 1: Parameters of the algorithms.

Algorithm	Parameter settings
PSO	Acceleration coefficients $c_1 = c_2 = 2$, inertia weight $\omega = 0.6$
WOA	Coefficient vector $a = [2, 0]$, logarithmic spiral shape constant $b = 1$
SSA	Discoverers PD = 20%, security threshold ST = 0.8, investigators SD = 10%
BOA	Sensory modality $c = 0.01$, power exponent $\alpha = 0.1$, switch probability $p = 0.6$
IBOA	Sensory modality $c = 0.01$, power exponent $\alpha = 0.1$

If $f(x_8) < f(x_3)$, the worst point x_3 is replaced by the shrinking point x_8. Otherwise, the worst point x_3 is replaced by the reflection point x_5.

3.2.4. IBOA Steps. In summary, the IBOA steps presented in this study can be expressed as follows:

Step 1: initialize parameters, using skew tent chaotic map to set population location;

Step 2: calculate the fitness value and record the initial extreme value;

Step 3: calculate the individual aroma size of each butterfly;

Step 4: perform global and local searches using formulas (19) and 20);

Step 5: improve the poor individuals by the simplex method;

Step 6: update the individual and global optimal solution of the butterfly;

Step 7: determine whether the algorithm has reached the maximum number of iterations and whether it has reached the end of the algorithm; otherwise, return to Step 3.

4. Test Function and Analysis

4.1. Parameter Settings. The 14 test functions are compared among PSO, WOA, SSA, BOA, and IBOA. The initial population size of all algorithms is set to 100, the number of iterations is 1000, each algorithm runs independently 30 times, and all simulations are completed on MATLAB 2019b. The algorithm parameter settings are shown in Table 1.

4.2. Test Function. The 14 benchmark test functions are selected for simulation analysis. The test function information is described in Table 2:

4.3. Algorithmic Test and Performance Comparison. The test results are described in Table 3.

The convergence curve is shown in Figure 2.

From the above results, IBOA is better than other algorithms in search accuracy and convergence speed, among which IBOA performs well in single-mode test functions f_1~f_5, can directly find the optimal value in f_1~f_4 test functions, and has the highest search accuracy in f_5 test functions compared with other algorithms. In the multimodal test functions f_6~f_{11}, IBOA still has a high optimization ability, in which the optimal values can be directly found in the test functions f_7 and f_9, and the convergence speed is faster than other algorithms. IBOA, BOA, and SSA search capabilities are almost the same in f_8 test functions, but IBOA has the advantage of faster convergence. In f_{10} and f_{11} test functions, IBOA has the highest accuracy and stability. In the fixed dimension test function f_{12}~f_{14}, each algorithm has excellent performance. In f_{12} and f_{14} test functions, all algorithms can quickly find the optimal value. In f_{13}, the optimization accuracy of IBOA and SSA is higher than that of other algorithms, and the convergence speed is faster. Through comparative experiments, IBOA solves the problem that BOA is easy to fall into local optimum and has poor convergence accuracy.

5. Simulation Results and Discussion

Three interconnected microgrids (MG1, MG2, and MG3) are selected for simulation analysis, in which a single microgrid is mainly composed of the PV, WT, DG, MT, ESS, and load. When dealing with microgrids, the multipower supplier preferentially supplies power to the one with more power shortages to improve overall economic benefits, and the calculation period is one day.

5.1. Case Parameters. Figure 3 shows the power generation of PV and MT and the load diagram required by the microgrid. Table 4 shows the power generation unit parameter, Table 5 demonstrates the environmental pollution parameter, Table 6 is the time-sharing electricity price table, and Table 7 illustrates the ESS parameter.

5.2. Result Analysis. Figure 4 shows the power output diagram of each power generation device based on the minimum total cost of the microgrid cluster under the island model. Figure 5 shows the power output diagram of each power generation device under the condition of grid connection. ESS discharge is preferred when PV and WT power generation is insufficient. When ESS reaches the lower discharge limit, the other power generation equipment with lower total cost takes precedence. The positive output value of ESS indicates discharge, while the negative output value indicates charge. The positive output values for the microgrid and the distribution network indicate the purchase of electricity, while the negative output values indicate the sale of electricity.

Table 2: Benchmark function.

Benchmark function	Dim	Range	Optima
$f_1 = \sum_{i=1}^{n} x_i^2$	30	[−100, 100]	0
$f_2 = \sum_{i=1}^{n} \lvert x_i \rvert + \prod_{i=1}^{n} \lvert x_i \rvert$	30	[−10, 10]	0
$f_3 = \sum_{i=1}^{n} (\sum_{j=1}^{i} x_j)^2$	30	[−100, 100]	0
$f_4 = \max_i \{\lvert x_i \rvert, 1 \le i \le n\}$	30	[−100, 100]	0
$f_5 = \sum_{i=1}^{n} i x_i^4 + \text{random}[0, 1)$	30	[−1.28, 1.28]	0
$f_6 = \sum_{i=1}^{n} -x_i \sin(\sqrt{\lvert x_i \rvert})$	30	[−500, 500]	$-418.98 * n$
$f_7 = \sum_{i=1}^{n} [x_i^2 - 10 \cos(2\pi x_i) + 10]$	30	[−5.12, 5.12]	0
$f_8 = -20 \exp(-0.2\sqrt{1/n \sum_{i=1}^{n} x_i^2}) - \exp(1/n \sum_{i=1}^{n} \cos(2\pi x_i)) + 20 + e$	30	[−32, 32]	0
$f_9 = 1/4000 \sum_{i=1}^{n} x_i^2 - \prod_{i=1}^{n} \cos(x_i/\sqrt{i}) + 1$	30	[−600, 600]	0
$f_{10} = \pi/n \left\{10 \sin(\pi y_1) + \sum_{i=1}^{n-1} (y_i - 1)^2 \times [1 + 10 \sin^2(\pi y_{i+1})] + (y_n - 1)^2\right\} + \sum_{i=1}^{n} u(x_i, 10, 100, 4)$ $y_i = 1 + x_i + 1/4,\ u(x_i, a, k, m) = \begin{cases} k(x_i - a)^m & x_i > a \\ 0 & -a < x_i < a \\ k(-x_i - a)^m & x_i < a \end{cases}$	30	[−50, 50]	0
$f_{11} = 0.1\left\{\sin^2(3\pi x_1) + \sum_{i=1}^{n} (x_i - 1)^2 [1 + \sin^2(3\pi x_i + 1)] + (x_i - 1)^2 + [1 + \sin^2(2\pi x_i)]\right\} + \sum_{i=1}^{n} u(x_i, 5, 100, 4)$	30	[−50, 50]	0
$f_{12} = (1/500 + \sum_{j=1}^{25} 1/j + \sum_{i=1}^{2} (x_i - a_{ij})^6)^{-1}$	2	[−65, 65]	1
$f_{13} = \sum_{i=1}^{11} [a_i - x_1 (b_i^2 + b_i x_i)/b_i^2 + b_i x_3 + x_4]^2$	4	[−5, 5]	0.00030
$f_{14} = [1 + (x_1 + x_2 + 1)^2 (19 - 14x_1 + 3x_1^2 - 14x_2 + 6x_1 x_2 + 3x_2^2)] \times [30 + (2x_1 - 3x_2)^2 (18 - 32x_1 + 12x_1^2 + 48x_2 - 36x_1 x_2 + 27x_2^2)]$	2	[−2, 2]	3

Table 3: Test results of different functions.

Function	Algorithm	Best	Avg	Std
f_1	PSO	$1.8539E-140$	$2.2126E-124$	$3.1259E-124$
	WOA	$1.2693E-201$	$3.8570E-195$	$0.0000E+00$
	SSA	$0.0000E+00$	$0.0000E+00$	$0.0000E+00$
	BOA	$4.2696E-105$	$1.4164E-103$	$1.8100E-103$
	IBOA	$0.0000E+00$	$0.0000E+00$	$0.0000E+00$
f_2	PSO	$5.0631E-70$	$1.3820E-61$	$1.9544E-61$
	WOA	$1.9255E-119$	$4.3549E-112$	$6.1533E-112$
	SSA	$0.0000E+00$	$0.0000E+00$	$0.0000E+00$
	BOA	$3.9626E-77$	$1.7330E-76$	$1.8012E-76$
	IBOA	$0.0000E+00$	$0.0000E+00$	$0.0000E+00$
f_3	PSO	$6.9869E-01$	$8.7387E-01$	$2.1321E-01$
	WOA	$2.5717E+03$	$4.0816E+03$	$1.1156E+03$
	SSA	$0.0000E+00$	$0.0000E+00$	$0.0000E+00$
	BOA	$8.9991E-105$	$4.0221E-104$	$2.4291E-104$
	IBOA	$0.0000E+00$	$0.0000E+00$	$0.0000E+00$
f_4	PSO	$1.0546E-65$	$1.8886E-61$	$2.6666E-61$
	WOA	$2.4586E+00$	$1.2221E+01$	$1.1671E+01$
	SSA	$0.0000E+00$	$0.0000E+00$	$0.0000E+00$
	BOA	$3.3476E-77$	$1.5992E-76$	$1.3416E-76$
	IBOA	$0.0000E+00$	$0.0000E+00$	$0.0000E+00$
f_5	PSO	$3.1796E-05$	$3.4680E-05$	$3.8048E-06$
	WOA	$5.5907E-05$	$2.0529E-04$	$1.3767E-04$
	SSA	$3.2522E-05$	$6.8277E-05$	$2.8181E-05$
	BOA	$2.3071E-06$	$5.9118E-06$	$2.7000E-06$
	IBOA	$1.6265E-09$	$6.1461E-08$	$4.2729E-08$
f_6	PSO	$-4.1898E+02$	$-4.1898E+02$	$0.0000E+00$
	WOA	$-1.2569E+04$	$-1.2206E+04$	$3.7103E+02$
	SSA	$-8.5591E+03$	$-7.9744E+03$	$5.1050E+02$
	BOA	$-2.9617E+03$	$-2.6778E+03$	$2.1900E+02$
	IBOA	$-2.1306E+04$	$-1.8067E+04$	$2.4580E+03$
f_7	PSO	$2.9000E+02$	$2.9000E+02$	$0.0000E+00$
	WOA	$0.0000E+00$	$0.0000E+00$	$0.0000E+00$
	SSA	$0.0000E+00$	$0.0000E+00$	$0.0000E+00$
	BOA	$0.0000E+00$	$0.0000E+00$	$0.0000E+00$
	IBOA	$0.0000E+00$	$0.0000E+00$	$0.0000E+00$
f_8	PSO	$1.6844E+00$	$1.6844E+00$	$0.0000E+00$
	WOA	$4.4409E-15$	$4.4409E-15$	$0.0000E+00$
	SSA	$8.8818E-16$	$8.8818E-16$	$0.0000E+00$
	BOA	$8.8818E-16$	$8.8818E-16$	$0.0000E+00$
	IBOA	$8.8818E-16$	$8.8818E-16$	$0.0000E+00$
f_9	PSO	$0.0000E+00$	$0.0000E+00$	$0.0000E+00$
	WOA	$0.0000E+00$	$0.0000E+00$	$0.0000E+00$
	SSA	$0.0000E+00$	$0.0000E+00$	$0.0000E+00$
	BOA	$0.0000E+00$	$0.0000E+00$	$0.0000E+00$
	IBOA	$0.0000E+00$	$0.0000E+00$	$0.0000E+00$
f_{10}	PSO	$6.3961E-01$	$6.3961E-01$	$0.0000E+00$
	WOA	$2.1848E-06$	$3.6203E-06$	$1.0209E-06$
	SSA	$1.8393E-18$	$6.8229E-17$	$1.0761E-16$
	BOA	$3.6084E-01$	$5.6215E-01$	$1.4293E-01$
	IBOA	$1.5705E-32$	$1.5705E-32$	$0.0000E+00$
f_{11}	PSO	$1.1309E+00$	$1.1309E+00$	$0.0000E+00$
	WOA	$1.1053E-03$	$8.3458E-03$	$5.1198E-03$
	SSA	$6.2205E-17$	$1.7189E-16$	$2.0162E-16$
	BOA	$2.4563E+00$	$2.8107E+00$	$2.5060E-01$
	IBOA	$1.3498E-32$	$1.3498E-32$	$0.0000E+00$
f_{12}	PSO	$9.9800E-01$	$9.9800E-01$	$0.0000E+00$
	WOA	$9.9800E-01$	$9.9800E-01$	$0.0000E+00$
	SSA	$9.9800E-01$	$9.9800E-01$	$0.0000E+00$
	BOA	$1.0014E+00$	$1.6017E+00$	$4.3285E-01$
	IBOA	$9.9800E-01$	$9.9800E-01$	$0.0000E+00$

Table 3: Continued.

Function	Algorithm	Best	Avg	Std
	PSO	1.4596$E-02$	1.4596$E-02$	0.0000$E+00$
	WOA	3.0757$E-04$	7.5286$E-04$	3.7988$E-04$
f_{13}	SSA	3.0749$E-04$	3.0749$E-04$	0.0000$E+00$
	BOA	3.5300$E-04$	4.0181$E-04$	4.0973$E-05$
	IBOA	3.0749$E-04$	3.0749$E-04$	0.0000$E+00$
	PSO	3.0000$E+00$	3.0000$E+00$	0.0000$E+00$
	WOA	3.0000$E+00$	3.0000$E+00$	0.0000$E+00$
f_{14}	SSA	3.0000$E+00$	3.0000$E+00$	0.0000$E+00$
	BOA	3.0000$E+00$	3.0000$E+00$	0.0000$E+00$
	IBOA	3.0000$E+00$	3.0000$E+00$	0.0000$E+00$

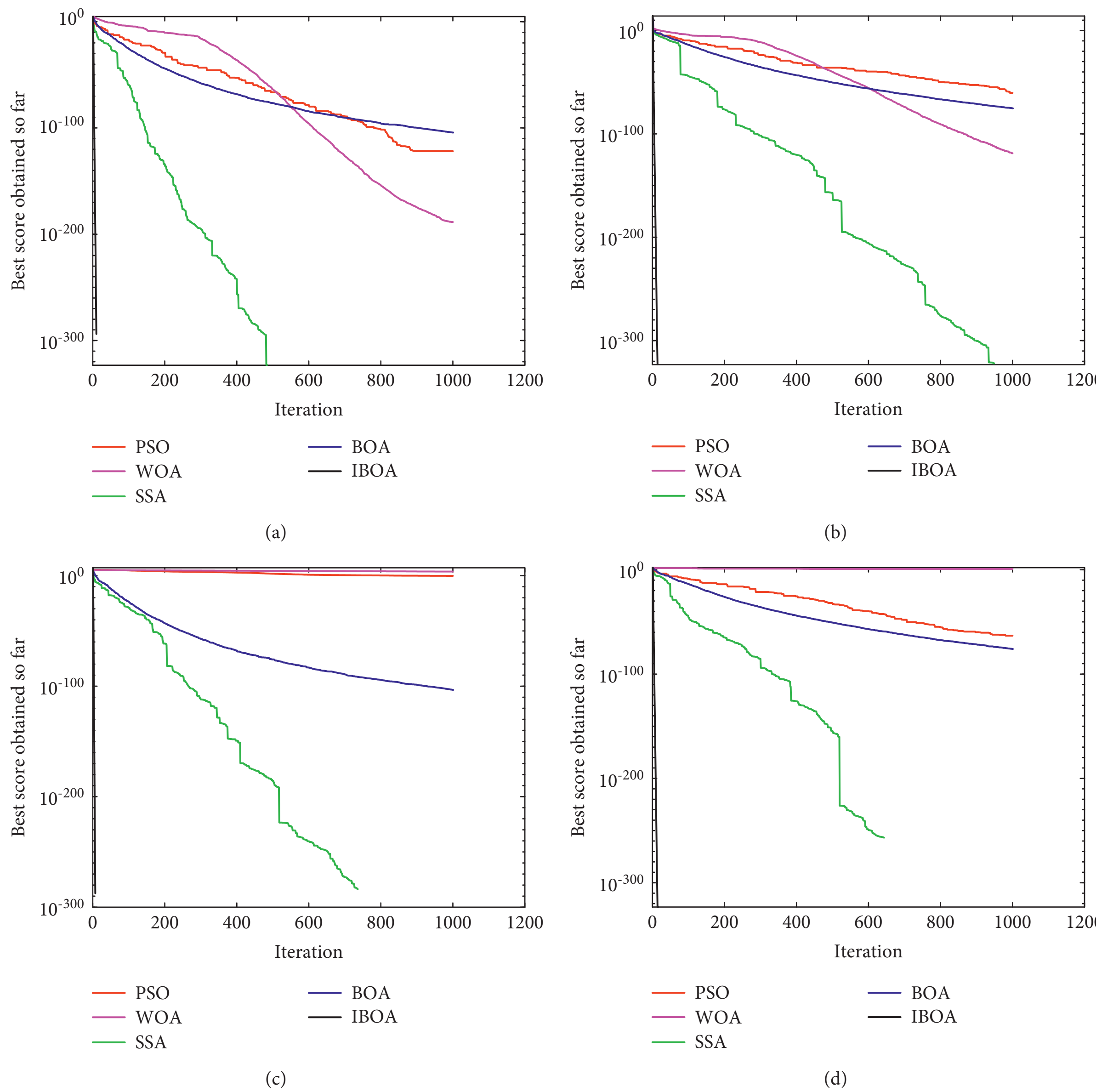

Figure 2: Continued.

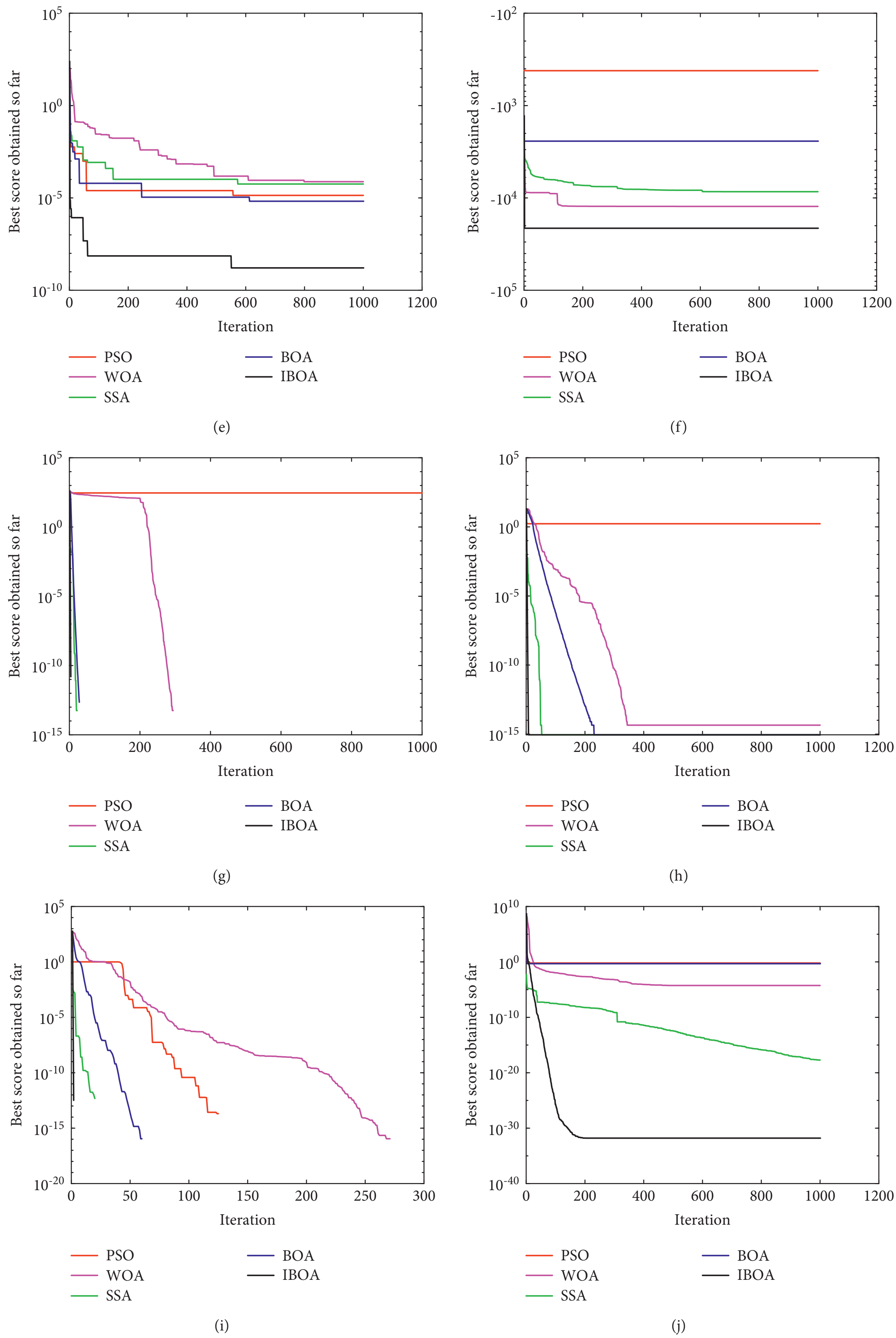

Figure 2: Continued.

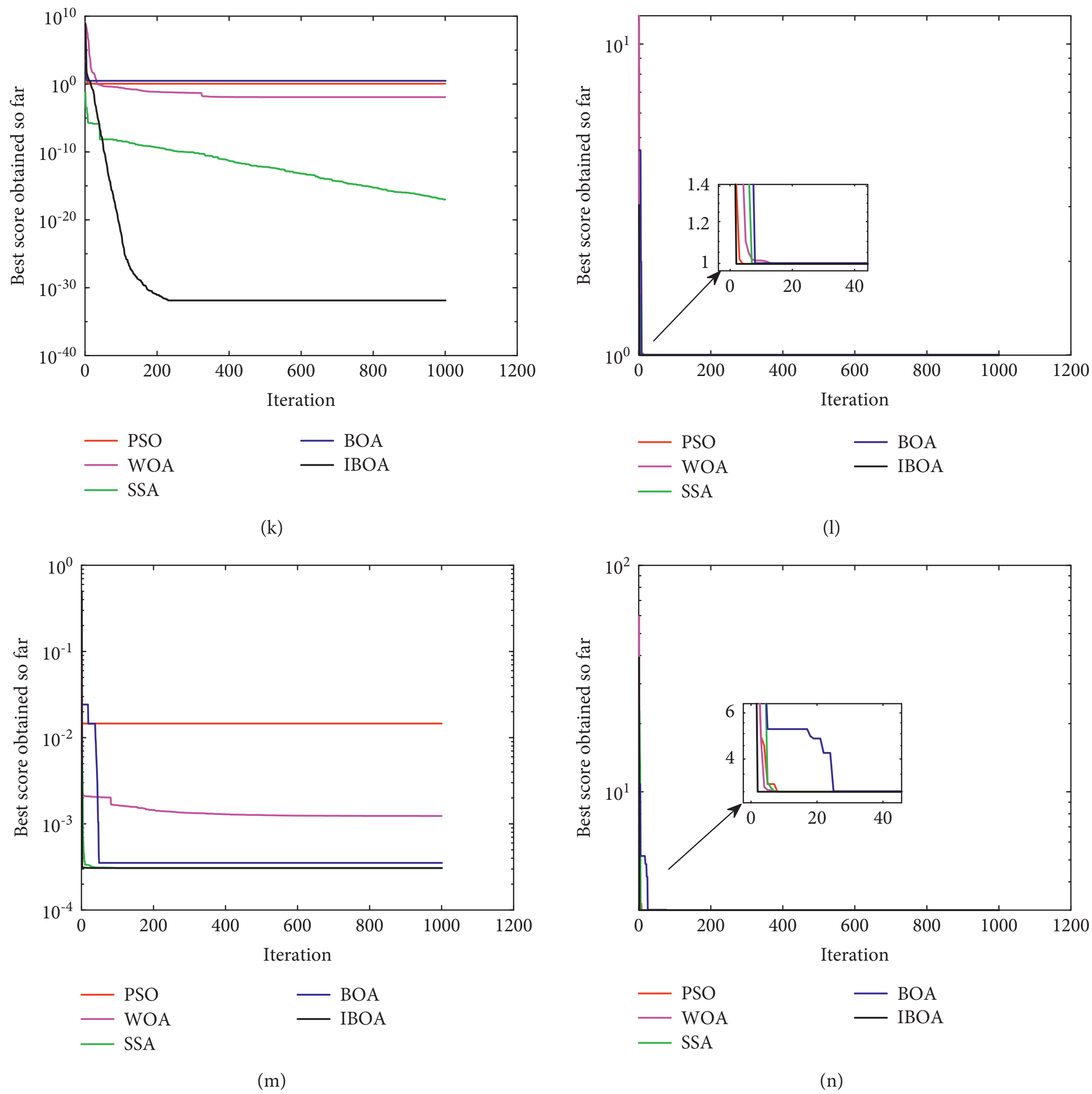

Figure 2: Function convergence diagram. (a) Convergence diagram of f_1. (b) Convergence diagram of f_2. (c) Convergence diagram of f_3. (d) Convergence diagram of f_4. (e) Convergence diagram of f_5. (f) Convergence diagram of f_6. (g) Convergence diagram of f_7. (h) Convergence diagram of f_8. (i) Convergence diagram of f_9. (j) Convergence diagram of f_{10}. (k) Convergence diagram of f_{11}. (l) Convergence diagram of f_{12}. (m) Convergence diagram of f_{13}. (n) Convergence diagram of f_{14}.

5.2.1. Economic Dispatch in the Island Model. Since the microgrid cluster is not connected to the distribution network in the island model, DG is used as the emergency power supply to provide the amount of electricity needed and remove the power constraint of DG to meet the power balance of the microgrid. The output of specific power generation equipment is shown in Figure 4.

Microgrid 3 is taken as an example, in 00:00–01:00, 05:00–08:00, and 20:00–24:00 time periods, the power generation is insufficient, and the amount of electricity lacking is first compensated by ESS, and after reaching the upper limit of ESS discharge, it is supplied by emergency power DG. In 02:00–04:00 and 09:00–19:00 periods, the power generation is sufficient and is charged to ESS, and after reaching the charge limit, the remaining electricity is sold to the power-deficit microgrid. Surplus power is sold to microgrid 2 in 03:00–04:00 time frame and microgrid 1 in 12:00–19:00 time frame. The microgrid cluster in the island model does not have the support of the distribution network, and DG is a high demand for itself as an emergency power supply.

5.2.2. Economic Dispatch in the Grid-Connected Model. The device output of the microgrid cluster in the grid-connected model is shown in Figure 5.

Microgrid 3 is taken as an example, in 00:00–01:00, 05:00–09:00, and 19:00–24:00 periods, the power generation is insufficient, and ESS discharge is given priority. When

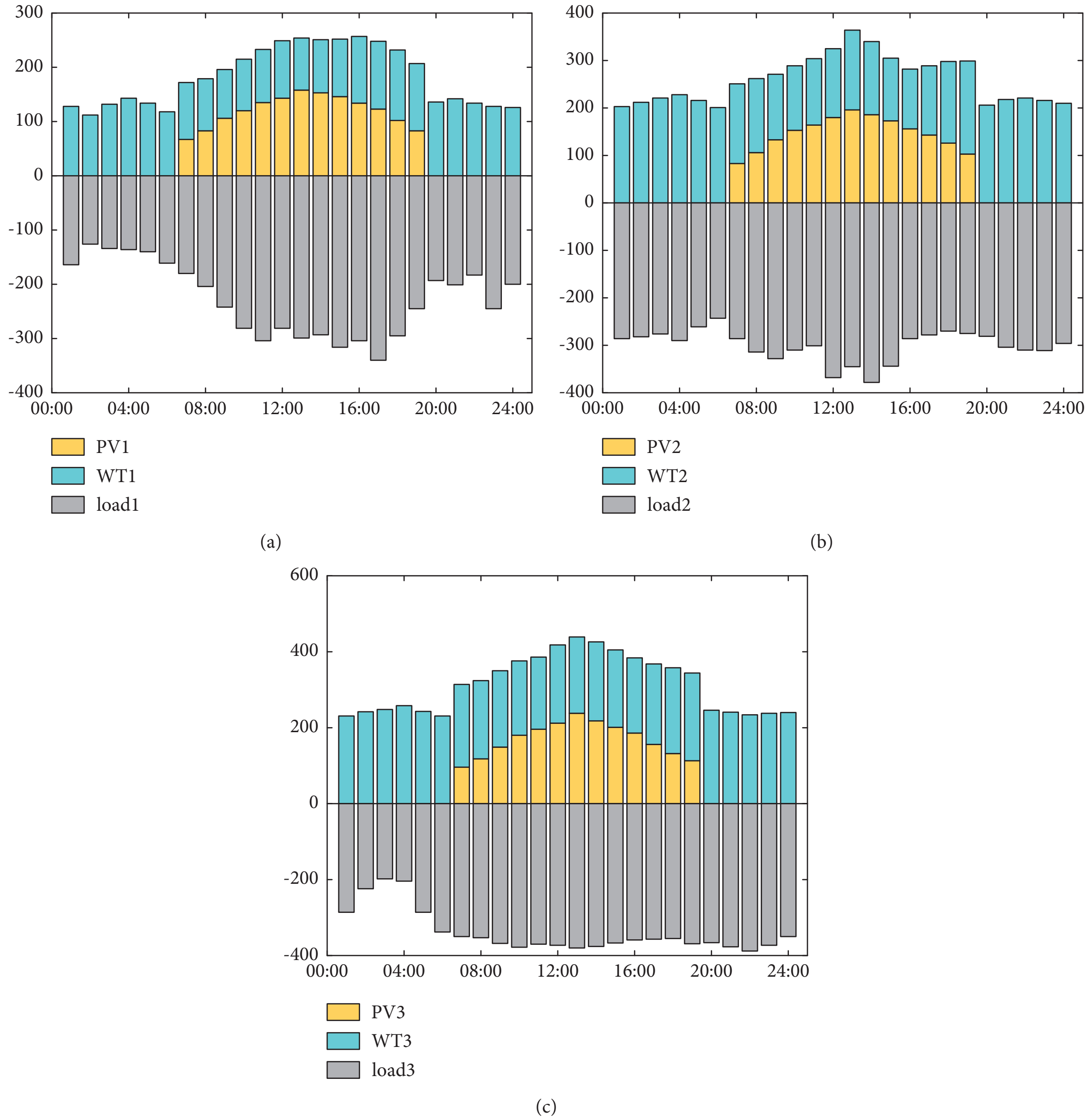

Figure 3: MG renewable energy and load forecasting. (a) MG1 prediction diagram. (b) MG2 prediction diagram. (c) MG3 prediction diagram.

Table 4: Parameters of power generation unit.

Equipment	Upper generation limit (kW)	Lower generation limit (kW)	Climb rate (kW/h)	Maintenance factor(CNY/kWh)
PV1	160	0	—	0.03
PV2	200	0	—	0.06
PV3	240	0	—	0.08
WT1	180	0	—	0.04
WT2	230	0	—	0.08
WT3	260	0	—	0.10
DG1	50	0	30	0.088
DG2	70	0	30	0.093
DG3	90	0	30	0.108
MT1	120	15	10	0.083
MT2	100	10	10	0.075
MT3	80	10	10	0.0648

Table 5: Pollution discharge factors and costs.

Type	Governance cost/(CNY/kg)	Pollutant discharge factor/(g/kWh)				
		PV	WT	DG	Grid	MT
CO_2	0.21	0	0	651	890	750
SO_2	14.85	0	0	0.218	1.92	0.041
NO_x	62.53	0	0	6.23	1.65	0.26

Table 6: Hourly electricity price.

Transaction form	Time interval		Distribution network	MG1	MG2	MG3
Sell electricity	Peak time	09:00–12:00 18:00–23:00	0.83	0.51	0.62	0.58
	Normal time	07:00–09:00 12:00–18:00	0.60	0.46	0.56	0.52
	Valley time	00:00–07:00 23:00–24:00	0.48	0.41	0.51	0.43
Purchase electricity		00:00–24:00	0.40	—	—	—

Table 7: Parameter settings for energy storage system.

Parameter	Value
Rated capacity/(kWh)	150
Maximum charge/discharge power/(kW)	50
Charge/discharge efficiency	0.9
Depreciation rate/(CNY/kW^2)	0.005
Installation cost/(CNY)	120000
Maximum/small charge capacity/(kWh)	135/30
Service life/year	10
Initial capacity/(kWh)	75

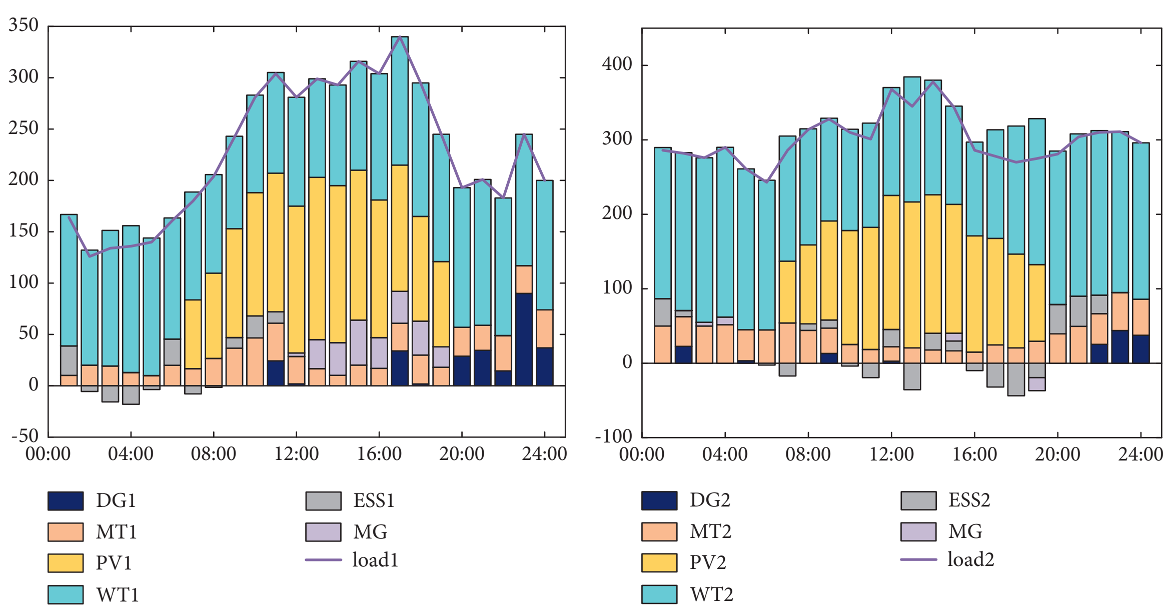

(a)

(b)

Figure 4: Continued.

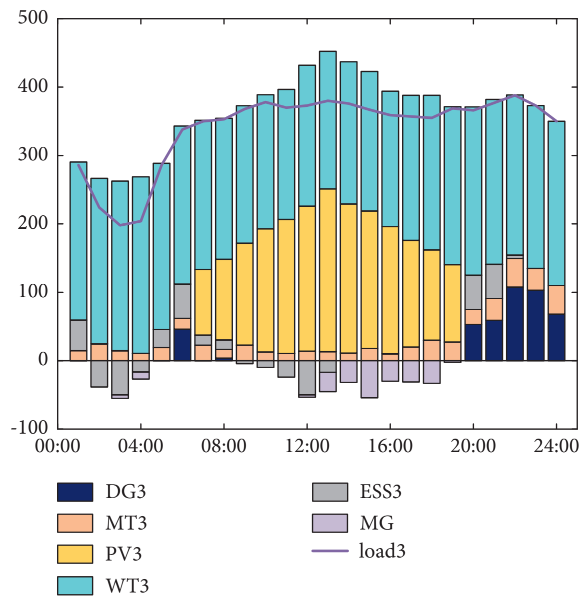

(c)

FIGURE 4: Equipment output in the island model. (a) MG1 equipment output diagram. (b) MG2 equipment output diagram. (c) MG3 equipment output diagram.

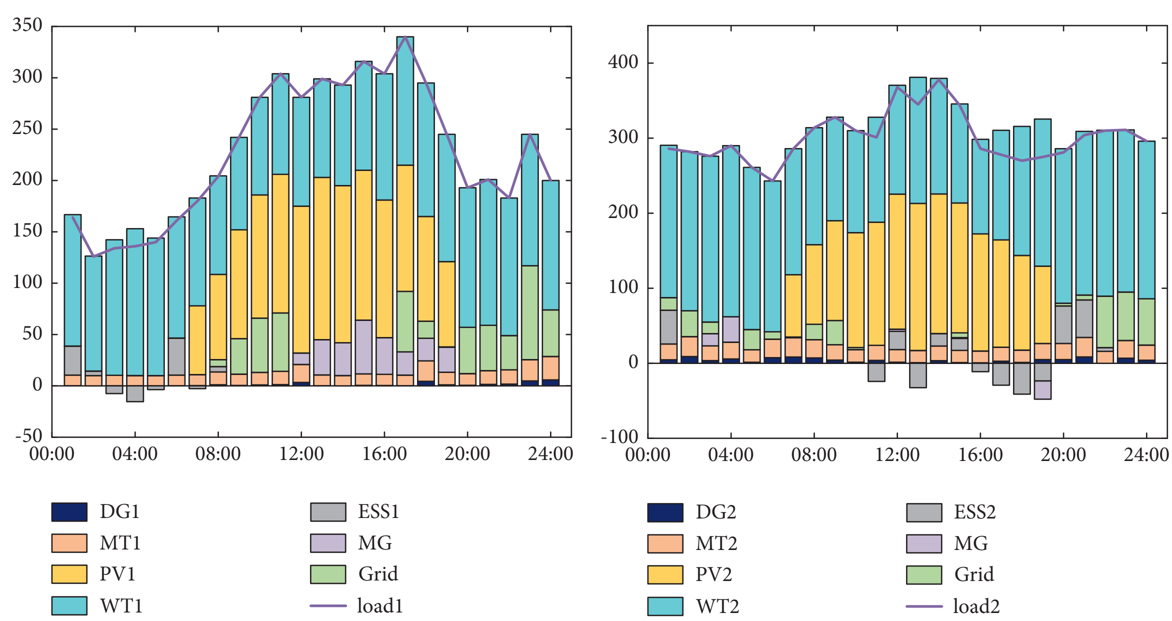

(a) (b)

FIGURE 5: Continued.

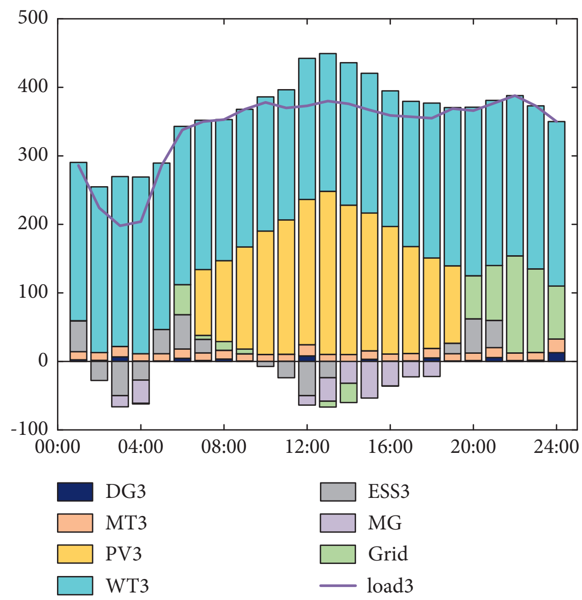

(c)

Figure 5: Equipment output in the grid-connected model. (a) MG1 equipment output diagram. (b) MG2 equipment output diagram. (c) MG3 equipment output diagram.

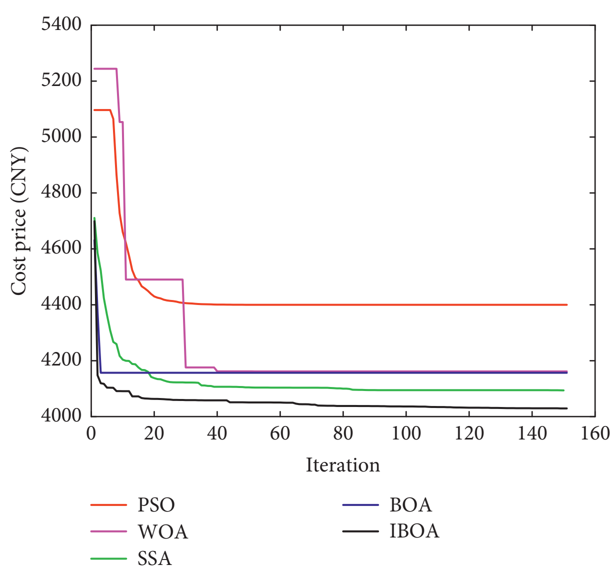

(a)

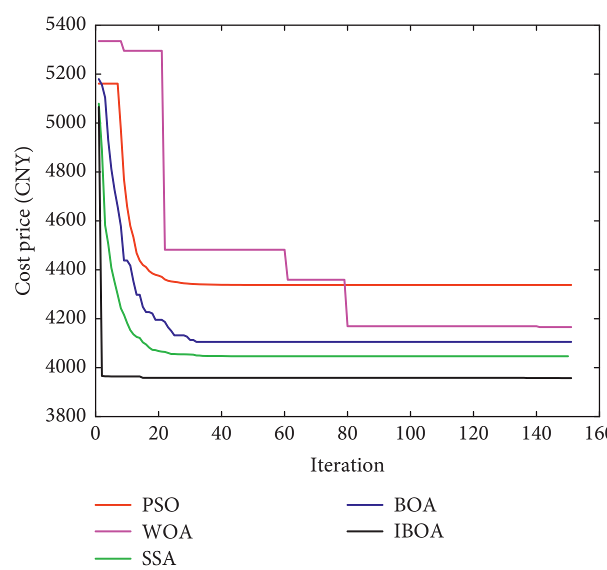

(b)

Figure 6: Algorithmic cost comparison. (a) Economic cost of the island model. (b) Economic cost of the grid-connected model.

ESS discharge reaches the upper limit, power purchase is made to the microgrid and distribution network. Since there is no excess power within the microgrid group in this period, power purchase is made to the distribution network to fill the shortage. In 02:00–04:00 and 10:00–18:00 periods, the power generation is sufficient, the excess power is charged to ESS, and then the remaining power is sold after reaching the maximum charge limit. Surplus power is sold to microgrid 2 in 03:00–04:00 time frame and microgrid 1 in 12:00–18:00 time frame. The power generation cost of MT is slightly lower than that of DG, and the power generation process can bring some heat, which can meet the resident's need for hot water and obtain additional benefits.

5.3. Analysis of Optimization Results. The result is shown in Figure 6. PSO, WOA, SSA, BOA, and IBOA are used to optimize the model, where Figure 6(a) is the economic cost in the island model and Figure 6(b) is the economic cost in the grid-connected model. In the grid-connected model, PSO cost is 4338.14 CNY, WOA cost is 4165.94 CNY, SSA cost is 4046.61 CNY, BOA cost is 4105.38 CNY, and IBOA cost is 3957.49 CNY. Among the costs of IBOA, the economic cost is 3343.39 CNY, and the environmental pollution cost is 614.11 CNY, and the economic cost includes the DG cost of 466.51 CNY, the MT cost of 557.18 CNY, the maintenance cost of PV and MT of 1421.20 CNY, the electric energy transaction cost of 538.07 CNY, and the ESS maintenance cost of 360.43 CNY. From the graph, IBOA is better than other algorithms in convergence speed and searchability.

6. Conclusions

This research constructs a microgrid cluster system model consisting of three single microgrids to solve the economic optimization dispatch problem. The information exchange center facilitates information sharing between single microgrids and between the microgrid cluster and the distribution network, and the model is simulated and solved by IBOA. To solve the problems of BOA falls into a local optimum easily and poor convergence accuracy, the skew tent chaotic map is used to initialize butterfly population, the Cauchy mutation is used to expand the search space, and the simplex method is used to improve the performance of the algorithm for poor individuals. The results of a comparison of 14 test functions with PSO, WOA, SSA, and BOA show that IBOA has significant advantages in terms of convergence speed and optimization accuracy. Finally, the proposed model is solved by simulation. Compared with other algorithms, IBOA has the highest economic benefit. By optimizing the microgrid cluster, the total operating cost is decreased, the dependence of the microgrid cluster on the distribution network is reduced effectively, and the development and utilization of renewable energy are promoted.

List of Symbols and Abbreviations

PV:	Photovoltaics
WT:	Wind turbine
MT:	Micro-turbine
ESS:	Energy storage system
DG:	Diesel generator
ET:	Electricity transaction
EM:	Equipment maintenance
C1:	The operating cost
C2:	The environmental pollution cost
c_i^{DG} and c_i^{MT}:	Generation cost of DG and MT
c_i^{EM}:	Operation and maintenance cost of PV and WT inside microgrid
c_i^{ESS}:	Operation cost of ESS
c_i^{ET}:	Electricity transaction cost
λ_k^{DG}, λ_k^{MT}, and $\lambda_k^{\mathrm{grid}}$:	Discharge factors of the K-type pollutants produced by DG, MT, and grid
P_i^{WT}, P_i^{PV}, P_i^{DG}, P_i^{MT}, and P_i^{ESS}:	Generated power of WT, PV, DG, MT, and ESS
k_i^{WT}, k_i^{PV}, k_i^{DG}, and k_i^{MT}:	Maintenance cost factors of WT, PV, DG, and MT
C_i^{cost}:	Total investment cost of ESS
P_i^{R}:	Rated power of ESS
T:	Annual running hours of ESS
d_i:	Depreciation rate of ESS
l_i:	Service life of ESS
P_i^{mg}:	Power for power trading between microgrids
P_i^{grid}:	Power for power trading between the microgrids and the distribution network
δ_i^{mg}:	Power price of microgrid
δ_i^{grid}:	Power price of the distribution networks
P_i^{load}:	Load size of the microgrid cluster system
$R_{i,\mathrm{up}}^{\mathrm{DG}}$, $R_{i,\mathrm{down}}^{\mathrm{DG}}$:	Up and down climb speed of DG
$R_{i,\mathrm{up}}^{\mathrm{MT}}$ and $R_{i,\mathrm{down}}^{\mathrm{MT}}$:	Up and down climb speed of MT
$\mathrm{SOC}_i^{\min}$ and $\mathrm{SOC}_i^{\max}$:	Minimum and maximum charges of the ESS
P_i^{ch}:	Charge power of ESS
P_i^{dis}:	Discharge power of ESS.

Data Availability

The data used to support the findings of this study are available from the corresponding author upon request.

Conflicts of Interest

The authors declare that they have no conflicts of interest.

Acknowledgments

This work was supported by the Open Research Fund of Guangxi Key Laboratory of Building New Energy and Energy Conservation (Gui Keneng 17-J-21-4).

References

[1] A. L. Bukar, C. W. Tan, L. K. Yiew, R. Ayop, and W.-S. Tan, "A rule-based energy management scheme for long-term optimal capacity planning of grid-independent microgrid optimized by multi-objective grasshopper optimization algorithm," *Energy Conversion and Management*, vol. 221, Article ID 113161, 2020.

[2] G. Hafeez, Z. Wadud, I. U. Khan et al., "Efficient energy management of IoT-enabled smart homes under price-based demand response program in smart grid," *Sensors*, vol. 20, no. 11, Article ID 3155, 2020.

[3] T. A. Khan, K. Ullah, G. Hafeez et al., "Closed-loop elastic demand control under dynamic pricing program in smart microgrid using super twisting sliding mode controller," *Sensors*, vol. 20, no. 16, Article ID 4376, 2020.

[4] N. Ghorbani, A. Kasaeian, A. Toopshekan, L. Bahrami, and A. Maghami, "Optimizing a hybrid wind-PV-battery system using GA-PSO and MOPSO for reducing cost and increasing reliability," *Energy*, vol. 154, pp. 581–591, 2018.

[5] S. Mohseni, A. C. Brent, and D. Burmester, "A demand response-centred approach to the long-term equipment

capacity planning of grid-independent micro-grids optimized by the moth-flame optimization algorithm," *Energy Conversion and Management*, vol. 200, Article ID 112105, 2019.

[6] W. Zhang, A. Maleki, M. A. Rosen, and J. Liu, "Sizing a stand-alone solar-wind-hydrogen energy system using weather forecasting and a hybrid search optimization algorithm," *Energy Conversion and Management*, vol. 180, pp. 609–621, 2019.

[7] M. Mohammadian, A. Lorestani, and M. M. Ardehali, "Optimization of single and multi-areas economic dispatch problems based on evolutionary particle swarm optimization algorithm," *Energy*, vol. 161, pp. 710–724, 2018.

[8] A. Ghasemi, H. Jamshidi Monfared, A. Loni, and M. Marzband, "CVaR-based retail electricity pricing in day-ahead scheduling of microgrids," *Energy*, vol. 227, Article ID 120529, 2021.

[9] Y. T. Shang, Y. C. Zheng, Z. Y. Shao, and L. Jian, "Computational performance analysis for centralized coordinated charging methods of plug-in electric vehicles: from the grid operator perspective," *Int Trans Electr Energ Syst*, vol. 30, Article ID e12229, 2020.

[10] P. Dhar and N. Chakraborty, "Optimal techno-economic analysis of a renewable based hybrid microgrid incorporating gravity energy storage system in Indian perspective using whale optimization algorithm," *Int Trans Electr Energ Syst*, vol. 31, Article ID e13025, 2021.

[11] D. Sadeghi, A. Hesami Naghshbandy, and S. Bahramara, "Optimal sizing of hybrid renewable energy systems in presence of electric vehicles using multi-objective particle swarm optimization," *Energy*, vol. 209, Article ID 118471, 2020.

[12] Y. F. Guo, X. T. Lei, and Q. Wang, "Capacity coordination planning of isolated microgrid and battery swapping station based on the quantum behavior particle swarm optimization algorithm," *Int Trans Electr Energ Syst*, vol. 31, Article ID e12804, 2021.

[13] P. Nagapurkar and J. D. Smith, "Techno-economic optimization and environmental Life Cycle Assessment (LCA) of microgrids located in the US using genetic algorithm," *Energy Conversion and Management*, vol. 181, pp. 272–291, 2019.

[14] T. T. Teo, T. Logenthiran, W. L. Woo et al., "Optimization of fuzzy energy-management system for grid-connected microgrid using NSGA-II," *IEEE Transactions on Cybernetics*, vol. 51, no. 11, pp. 5375–5386, 2021.

[15] W. Dong, Y. Li, and J. Xiang, "Optimal sizing of a stand-alone hybrid power system based on battery/hydrogen with an improved ant colony optimization," *Energies*, vol. 9, no. 10, p. 785, 2016.

[16] D. Miao and S. Hossain, "Improved gray wolf optimization algorithm for solving placement and sizing of electrical energy storage system in micro-grids," *ISA Transactions*, vol. 102, pp. 376–387, 2020.

[17] A. Lorestani, G. B. Gharehpetian, and M. H. Nazari, "Optimal sizing and techno-economic analysis of energy- and cost-efficient standalone multi-carrier microgrid," *Energy*, vol. 178, pp. 751–764, 2019.

[18] T. S. Mahmoud, B. S. Ahmed, and M. Y. Hassan, "The role of intelligent generation control algorithms in optimizing battery energy storage systems size in microgrids: a case study from Western Australia," *Energy Conversion and Management*, vol. 196, pp. 1335–1352, 2019.

[19] A. L. Bukar, C. W. Tan, and K. Y. Lau, "Optimal sizing of an autonomous photovoltaic/wind/battery/diesel generator microgrid using grasshopper optimization algorithm," *Solar Energy*, vol. 188, pp. 685–696, 2019.

[20] A. Sahoo and P. K. Hota, "Impact of energy storage system and distributed energy resources on bidding strategy of micro-grid in deregulated environment," *Journal of Energy Storage*, vol. 43, Article ID 103230, 2021.

[21] Z. Younes, I. Alhamrouni, S. Mekhilef, and M. Reyasudin, "A memory-based gravitational search algorithm for solving economic dispatch problem in micro-grid," *Ain Shams Engineering Journal*, vol. 12, no. 2, pp. 1985–1994, 2021.

[22] S. Mohseni, A. C. Brent, D. Burmester, and W. N. Browne, "Lévy-flight moth-flame optimisation algorithm-based micro-grid equipment sizing: an integrated investment and operational planning approach," *Energy and AI*, vol. 3, Article ID 100047, 2021.

[23] M. Zolfaghari, N. Ghaffarzadeh, and A. J. Ardakani, "Optimal sizing of battery energy storage systems in off-grid micro grids using convex optimization," *Journal of Energy Storage*, vol. 23, pp. 44–56, 2019.

[24] L. He, H. F. Lyu, J. F. Li, and L. C. Yu, "Research on optimal scheduling of microgrid energy based on SA_AFSA," *Acta Energiae Solaris Sinica*, vol. 41, no. 9, pp. 36–43, 2020.

[25] S. Cheng, Z. M. Chen, R. Wang, J. Heli, and B. W.eizhao, "Double-layer coordinated optimal dispatching of multi-microgrid based on mixed game," *Electric Power Automation Equipment*, vol. 41, no. 8, pp. 41–46, 2021.

[26] S. Arora and S. Singh, "Butterfly optimization algorithm: a novel approach for global optimization," *Soft Computing*, vol. 23, no. 3, pp. 715–734, 2019.

[27] H. Chen, M. Wang, and X. Zhao, "A multi-strategy enhanced sine cosine algorithm for global optimization and constrained practical engineering problems," *Applied Mathematics and Computation*, vol. 369, Article ID 124872, 2020.